Deriving Camera and Lens Settings for Fixed Traffic Enforcement and ALPR Cameras

A. Makarov*†, V. Lukić* and M. Španović*†
* R&D Centre Vlatacom, Belgrade, Serbia
† Faculty of Technical Sciences, University of Novi Sad, Serbia
Aleksej@vlatacom.com, Milana.Spanovic@vlatacom.com, Vojislav.Lukic@vlatacom.com

***Abstract*—A methodology for computing parameters of fixed ALPR and traffic enforcement cameras is presented. The minimum spatial resolution of the camera is defined on the basis of license plate font analysis. A camera calibration model is used to measure dimensions of the area of interest. The camera pose is analyzed with the objective of minimizing occlusion and maximizing the number of frames containing the infringing vehicle. The optimal focal length of the lens is computed based on the scene and sensor dimensions. The lens aperture is set in a way that optimizes the sharpness and brightness of license plates in the area of interest. The minimum shutter speed is defined in order to cope with fast moving vehicles. This approach has been confirmed in practice in configuring the traffic enforcement system of the city of Belgrade.**

I. INTRODUCTION

Cameras are widely used in traffic enforcement. In this application area, a camera is expected to fulfill two basic requests:

- Irrefutable proof of traffic violation;
- Unambiguous identification of the traffic offender.

For these objectives to be reached, the camera should provide a number of frames containing a sharp and sufficiently sized projection of the perpetrating vehicle.

The sharpness and the relative size of the projection of an object onto the image sensor is related to its distance from the camera and to the focal length and the aperture of its lens. The image sensor exposure time also influences the image sharpness of the vehicles involved in moving violations. The sensor size, resolution, frame rate, exposure and field of view should be set in a way that the vehicle identification features caught by a camera are distinct at the highest expected vehicle speed.

The process of determining the optical and geometric parameters of a camera and its lens with respect to the outside world is usually referred to as calibration. The related literature distinguishes between two kinds of quantities to be calibrated: the extrinsic and intrinsic parameters [1]. The *extrinsic* parameters are defined as those defined by the camera position in the outside world: the camera height above the ground, its horizontal distance from the road (if any) and the lane width, the camera inclination angle towards the road (the tilt or pitch), its deviation angle from a line parallel to the road (the pan or azimuth) and the angle which represents the deviation of the camera "vertical" axis from the outside world vertical axis (the roll or swing).

This work is partially supported by the following grant: "Innovative electronic components and systems based on inorganic and organic technologies embedded in consumer goods and products", Project No TR32016, Serbian Ministry of Education and Science.

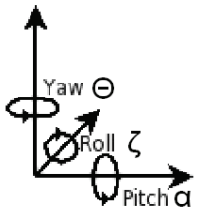

Figure 1. Possible camera rotation angles (from http://sidvind.com/wiki/Yaw,_pitch,_roll_camera)

In urban conditions, the choice of extrinsic parameters is reduced by local building regulations and by cost optimization. Namely, the local building regulations usually prescribe the minimum height at which a camera can be mounted above the pavement, in order not to impede the traffic. Other extrinsic parameters are influenced by permitting, the road geometry, the position of the area of interest and the available infrastructure. The latter is imposed by local regulators, who often request the cameras be mounted on existing poles or gantries, as well as for the purposes of the project cost optimization, which requires installation in the vicinity of existing power and network nodes. In addition, when traffic violations are detected in conjunction with other sensors, such as radars or road sensors, the range of possible tilt and pitch angles is further reduced. The roll angle can be set to zero in order to align the sensor with the outside world vertical axis. Thus, the external parameters are imposed by external factors and not by optimum performance objectives. The values of extrinsic parameters are accurately measure d with laser rangefinders and goniometers. This paper focuses on camera and lens parameters, such as the sensor size and resolution, the focal length and aperture, should be derived in a way to meet the challenges of the outside world. These internal camera geometric and optical characteristics are usually referred to as *intrinsic* parameters [1].

The research on computer vision in the areas of robotics and stereoscopy established models for mapping the 3D world spatial characteristics to planar coordinates and vice versa [1]-[7]. This mapping enables calibration of both extrinsic and intrinsic spatial parameters. Namely, the perspective projection models adopted are fairly general and offer the possibility of reconstructing the 3D metrics,

2D coordinates, the focal length and the camera pose information from multiple views made either with a moving or a stereoscopic camera [6],[7]. Alternatively, a fixed monocular camera can be calibrated using multiple views and poses of calibration patterns with known geometric properties [8], [9].

In this paper, the main parameter for calibrating a camera is the visibility of the characters of its license plates. We shall define rules for covering the road area of interest, based on the camera pose and its intrinsic parameters, both spatial (sensor resolution, sensor size, the focal length and aperture of the lens) and temporal (camera shutter speed, frame rate). Here, the area of interest is defined as a part of the road (i) in which the license plates are recognizable by a human observer or automaton, and (ii) which is long enough for providing irrefutable proof of violation.

II. LICENSE PLATE FONT ANALYSIS

Before deploying an ALPR based traffic enforcement system in a country or state, it is important to analyze the properties of license plates. In European countries, ALPR systems are usually expected to read both domestic and foreign license plates. Most European countries use *DIN-1451* derived fonts. E.g., this font is with some variations used in Austria, Belgium, Croatia, Czech Republic, Finland, Hungary, Italy, Poland, Romania, Slovakia, Spain and Sweden [12]. New Serbian plates are based on a similar but narrower *FF DIN Condensed* font. Figs. 2-4 show most widely used license plate fonts, while Table 1 gives and overview of the character dimensions.

Figure 2. British license plate font (Charles Wright 2001)

Figure 3. German plate font (Fälschungserschwerende Schrift)

Figure 4. Serbian plate font (FF DIN Condensed)

Table 1. Dimensions of characters on license plates issued by UK, Germany, Croatia and Serbia

Character dimensions :	H [mm]	W [mm]	W (Numerals)	Stroke [mm]	Area per char. [mm^2]
UK	79	50	50	14	3950
Germany	75	40.5-49	38.5	14	2887-3675
Croatia & pre-2011 Serbia (DIN 1451)	74	40	40	9	2960
Serbia after 2011	75 80 w/ accents	36	31	11 5 for accents	2325-2700

Free flow of people and goods requires technological updates of ALPR and traffic enforcement systems. A license plate capturing system should be able to accurately record the smallest significant details on a wide range of international license plates encountered on European roads. From Table 1, it is obvious that characters on new Serbian plates occupy significantly less area than characters on other plates. Characters on British, German and pre-2011 Serbian plates occupy up to 70%, 36% and 27% more area, respectively, than new Serbian characters without diacritical marks. A system designed and calibrated solely for British or German plates might have insufficient spatial resolution for capturing diacritical marks on letters "**Č**", "**Ć**", "**Đ**", "**Š**" and "**Ž**" on new Serbian license plates. These letters have 5 mm high accents embossed with 5 mm stroke. Their misinterpretation, due to insufficient resolution, noise, dirt, wear or forging, would give rise to false character classification. For example, letter "**Č**" can be read as "**C**", and vice versa. while the bar in letter "**Đ**" is barely visible and easily confused with "**D**". Such errors lead to false identification of a vehicle. Taking into account the minimum stroke on license plates is 5 millimeters, as is the minimum height of diacritical marks, the critical sampling distance (i.e., the inverse of the Nyquist sampling rate), above which the character details would be omitted and aliased, is 5 millimeters. In order to avoid a loss of information due to noise and to non-optimal stroke orientation, we should sample characters with at least two samples per stroke. Thus, we shall set the minimum sampling frequency to one half of the character sampling Nyquist rate, i.e. $\rho_{min} = 2.5$ mm/pel. This is equivalent to a minimum linear resolution of 32 pixels per character on new Serbian license plates (from Table 1, a character with accent is 80 mm high).

Based on the sensor size, the number of pixels and on the focal length of its lens, it easy to compute the maximum distance at which the linear resolution will be greater or equal to ρ_{min}, Fig. 5 shows this distance, D_{max}, can be computed from the camera angle of view φ, which will be shown below to be a function of the aforementioned intrinsic parameters.

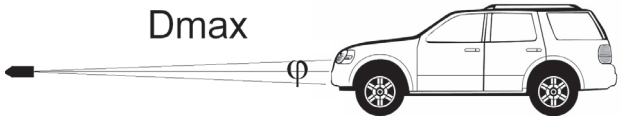

Figure 5. Measuring the maximum distance for reading characters.

From Fig.6, one can see that a character of height h_c projects an image of approximate size

$$h_i = \frac{n_r}{N_r} h_{s,}$$

where n_r is the number of rows over which its image spreads, N_r is the total number of rows in the sensor, and h_s is the sensor height. This approximation is valid as long as $N_r >> n_r$. From Fig.5, a character at distance D, projects an image at the focal point of the lens, i..e., at distance equal to the focal length f:

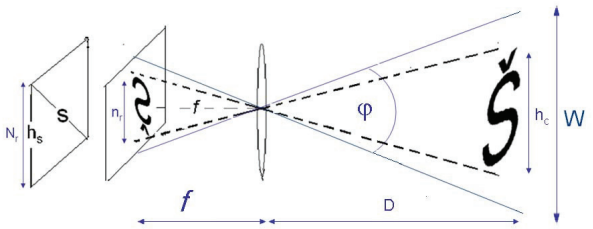

Figure 6. Projection of a letter with diacritical mark of height h_c onto the s sized sensor over n_r rows

From vertically opposite angles in Fig.5,

$$\frac{h_c}{D} = \frac{\frac{n_r}{N_r} h_s}{f},$$

the maximum distance is

$$D_{\max} = f \frac{N_r}{h_s \rho_{\min}} \qquad (1)$$

For example, the maximum distance at which license plates are readable with ρ_{min} = 2.5mm/pel, for a camera sensor of h_s=3.6mm height (i.e., sensor size of s = ⅓"), N_r=960 rows, and the lens of focal length f=25mm, is according to Eq.1, D_{max}=16.7 meters.

III. CAMERA POSE IN DENSE TRAFFIC CONDITIONS

A camera mounted at the height of a license plate with zero tilt, as in Fig.5, allows for automated character recognition at maximum distances, but only for isolated vehicles. In urban conditions, due to traffic density, infringing vehicles can be occluded by preceding or trailing vehicles. Consequently, the camera external parameters should be adjusted with respect to those in Fig.5 in order to cope with the risk of vandalism and occlusion. In such conditions, the camera should be installed at a safe height H, and point to vehicles at a tilt angle α in order to capture a license plate while not occluded by a neighboring vehicle. The angle α should be a function of the inter-vehicle spacing Δ_g and of the average vehicle height h_v,

$$\alpha = \arctan(\frac{H_{v_v}}{\Delta_g}) \qquad (2)$$

as shown in Fig.7. For moving violations, at speeds above 50 km/h (13.9 m/s), inter-vehicle gap Δ_g is usually above 5 meters, as shown in Fig.8 [13]. The same inter-vehicle spacing value has been reported in congested traffic [14]. This minimum spacing corresponds to the distance traveled at minimum reaction time of about 0.5 seconds [15]. Assuming H_v=3.2m (a bus) and Δ_g is 5 meters, angle α is 32.6˚. Gaps between vehicles at higher speeds are usually larger, hence the tilt α can sometimes be reduced to even 20˚, at which a license plate maximum distance is Δ_g = 8.8 meters away from the bus edge or 4.4 meters away from a passenger vehicle edge, according to (2) .

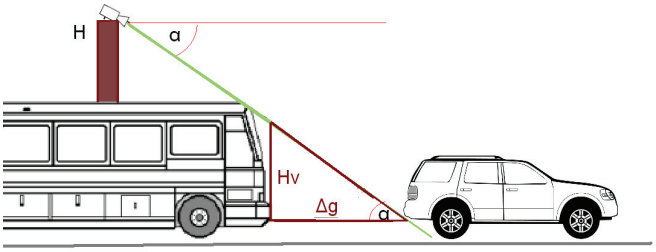

Figure 7. Gap between vehicles, height of the trailing vehicle and camera tilt. Optimal α is about 30˚.

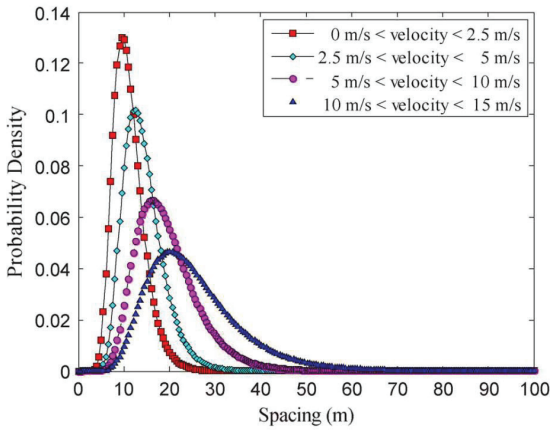

Figure 8 Spacing between vehicles at different velocities [13]

IV. COVERING THE AREA OF INTEREST

In this Section, in order to predict the area of interest covered by a camera with given intrinsic and extrinsic parameters, we shall establish the perspective projection model of the outside world as seen by a pinhole camera with a thin distortionless lens. The projection of the road scene onto the image sensor is modeled by 9 extrinsic and intrinsic parameters. For simplicity, the imaging system model is reduced to four camera pose parameters: tilt angle α, pan angle θ, the height H, and the horizontal distance between the camera and the middle of the lane L. The roll (swing) angle ζ of the camera has been assumed to be zero, i.e., the sensor lower edge is assumed to be perfectly parallel to the surface of the road. This feature is desirable and allows for aligning the outside world with its projection displayed on screens. As mentioned above, the roll angle can be adjusted by laser goniometers. For perspective projection considerations, we retain 5 intrinsic parameters: the focal length f, the sensor height h_s, the sensor width w_s, the number of rows N_r and the number of columns N_c in the sensor matrix. Fig.9 provides the road-side view of the imaging system and the outside world.

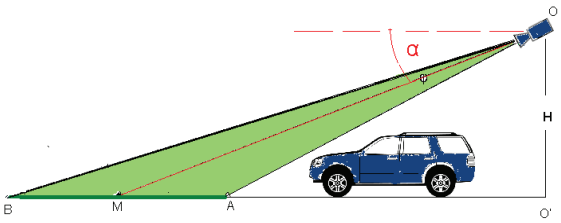

Figure 9. Roadside view: a vehicle entering the camera ray of width φ_h.

From Fig.9, the length of the road captured by the area is computed as:

$$AB = O'B - O'A = H \cdot \left[\cot(\alpha - \frac{\varphi_h}{2}) - \cot(\alpha + \frac{\varphi_h}{2}) \right] \quad (3)$$

Where H denotes the camera height, α is the camera tilt and φ_h is the angle of view in the direction of the sensor height. The angle of view φ_h can be computed from Fig.10, as

$$\varphi_h = 2\arctan(\frac{h_s}{2f}) \quad (4)$$

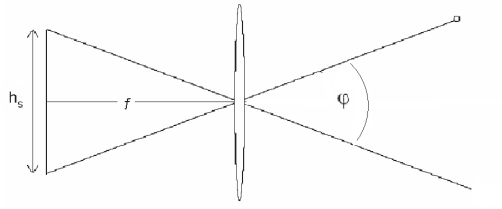

Figure 10. Field of view and intrinsic parameters

Similarly, from Fig.11, the sides of a trapezoid delimiting the area of interest can be computed as

$$MN = 2 \cdot MA = 2 \cdot O'A \cdot \tan(\frac{\varphi_w}{2}) = \\ = 2 \cdot H \cdot \tan(\frac{\varphi_w}{2}) \cdot \cot(\alpha + \frac{\varphi_h}{2}) \quad (5)$$

$$PQ = 2 \cdot MA = 2 \cdot O'B \cdot \tan(\frac{\varphi_w}{2}) = \\ = 2 \cdot H \cdot \tan(\frac{\varphi_w}{2}) \cdot \cot(\alpha - \frac{\varphi_h}{2}) \quad (6)$$

$$MP = NQ = O'P - O'M = \\ 2 \cdot H \cdot \sec(\frac{\varphi_w}{2}) \cdot \left[\cot(\alpha - \frac{\varphi_h}{2}) - \cot(\alpha + \frac{\varphi_h}{2}) \right] \quad (7)$$

In order to cover the maximum length S of the road, the pan angle θ should be as small as possible.

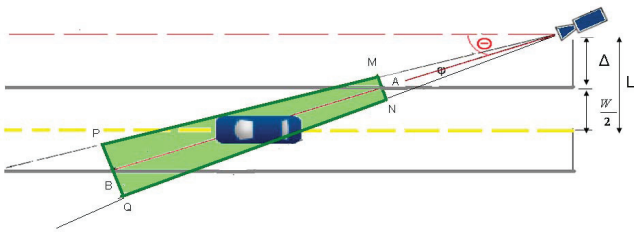

Figure 11., *Top view of a vehicle entering the camera ray of width* φ_w.

$$S = AB \cdot \cos\theta = \\ H \cdot \left[\cot(\alpha - \frac{\varphi_h}{2}) - \cot(\alpha + \frac{\varphi_h}{2}) \right] \cdot \cos\theta \quad (8)$$

Obviously, the best coverage is provided by over-the-lane cameras, where θ can be set to zero.

The trapezoid MNQP representing the scanned area of the outside world is projected onto the image sensor M'N'Q'P', as shown in Fig.12. As this trapezoid is projected to a rectangle, it gives rise to perspective (parallel lines in the outside world converge in the image).

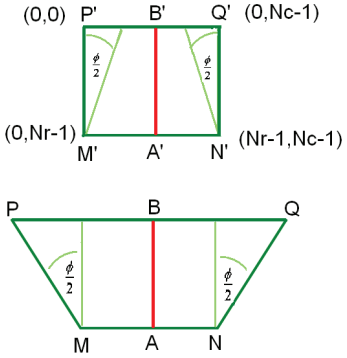

Figure 12. The projection of the trapezoidal field of view MNQP (bottom) onto the image sensor matrix (top).

V. OPTIMAL FOCAL LENGTH FOR A ROAD SECTION

The focal length of a lens covering a desired distance AB shown in Fig.9 and defined by equations (3) and (4), can be computed given the sensor size, tilt and height. A column of pixels in the sensor and the road section are here assumed to be in the same plane, i.e. θ= ζ =0.

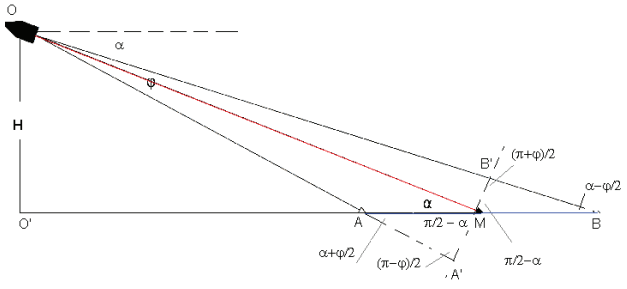

Figure 13. Angle of view φ and the focal length f determined from the target section AB, camera height H and tilt α.

The exact solution for the angle of view φ, and consequently for the focal length *f* according to Eq. 4, is a set of quartic equation roots derived from trigonometric transformations applied to triangles in Fig.13. An approximation, valid as long as φ << α, can be applied, by observing that the angle of view φ in the scene shown in Fig.13 is vertically opposite to the one inside the camera, shown in Fig.10,

$$\frac{A'B'}{OM} = \frac{h_s}{f} \tag{9}$$

where OM is the distance of the mid-section point M from the camera, and A'B' is the linear field of view. The section AB projects on A'B' and consequently onto the entire sensor. The approximation here lies in the assumption that the angle between the camera ray and the road surface is equal to the tilt angle α, while in reality it varies form (α-φ/2) to (α+-φ/2). By substituting A'B' = L sin(α), and OM = H/sin(α), the focal length *f* is

$$f = \frac{h_s H}{L \cdot \sin^2 \alpha} \tag{10}$$

For typical values, such as 1/3" sensor (i.e., sensor height of 3.6mm), camera height of 5 meters and tilt of 30˚, the distance of L=10 meters would spread over the entire sensor height with a focal length of 7.2 mm. An off-the-shelf choice for such a scene would probably be a 8mm lens.

VI. Optimal Aperture and Depth of Field

The traffic enforcement and ALPR cameras should track the vehicles and license plates throughout the scene with high visual acuity. Then the lens should be focused to infinity, which means that the lens-maker formula can be simplified as follows,

$$\frac{1}{d} + \frac{1}{i} = \frac{1}{f} \quad \underset{d \to \infty}{\Longrightarrow} \quad i = f \tag{11}$$

where *d* is the distance of the object from the lens, *i* is the distance of the image from the lens, and *f* is the focal length. Equation (11) shows that for distant objects to be focused, the image sensor should be put in the lens focus. For ALPR to work properly, it is important to ensure that the whole scene is focused, i.e., that the minimum distance from the lens at which the objects are focused is less than the distance OA in Fig.9.

The depth of field is adjusted by setting the diameter of the lens aperture to an appropriate value *A*. Namely, the aperture is the adjustable opening in the lens, which, besides controlling the amount of light that enters the sensor, defines the range of distances in the scene.

The upper part of Fig.14 shows the arrangement of the lens and the sensor as described by (11). The lower part of Fig.14 shows the same arrangement, but with an object at a close distance d_0, projecting an image at distance $i \neq f$, i.e. f-i away from the sensor. This image projects a circle of diameter *c* on the sensor, which is equivalent to a blur whose extent we want to keep below perception. This means that *c* should be of sub-pixel size. By observing vertically opposite angles in the bottom part of Fig. 14,

$$\frac{A}{i} = \frac{c}{f-i} \text{ and } \frac{1}{d_0} + \frac{1}{i} = \frac{1}{f} \Rightarrow A = \frac{c \cdot d_0}{f} \tag{12}$$

Since the aperture is usually expressed through its "F-number", *N*, where $A = f / N$, we can write (12) as

$$N = \frac{f^2}{d_0 \cdot c} \tag{13}$$

In Fig.13, $d_0 = OA = H \sec(\alpha + \varphi/2)$. The pixel height can be expressed as h_s / N_r.

$$N = \frac{f^2 \cdot N_r \cdot \cos(\alpha + \arctan(\frac{h_s}{2f}))}{H \cdot h_s} \tag{14}$$

Assuming *H*=5 meters, α = 30, *f*=16mm, h_s=3.6mm and N_r=960 , we obtain *N*=11. Consequently, the aperture should be set to *A*=*f*/*N*=*f*/11 in order to have maximum brightness with sharpness everywhere in the scene.

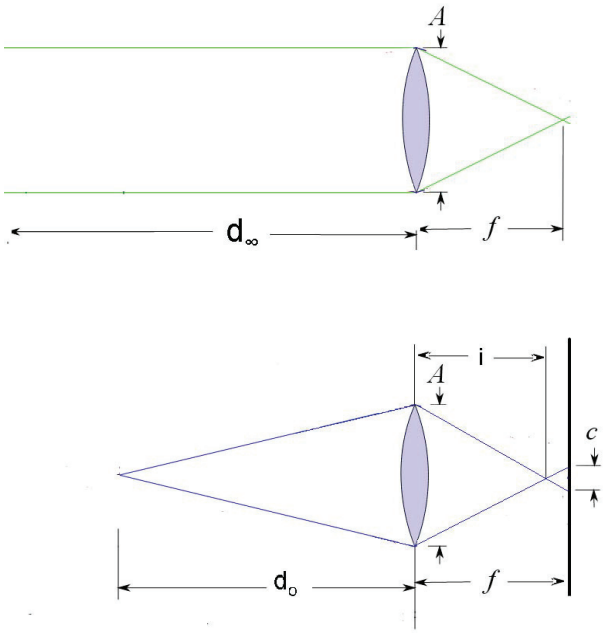

Figure 14. Projection of infinitely distant (top) and close objects (bottom).

VII. MAXIMUM DETECTABLE VEHICLE SPEED

When detecting speed violations, at least two frames are necessary to underpin the speed measurement record with visual evidence. Theoretically, if a vehicle is moving too fast, it can cross the whole visual scene MNQP in Fig.11, after the last and before the new frame capture. For the given camera frame rate r, and the observed road section of length S, given by Eq.8, the maximum detectable speed can be computed as

$$v_{\max} = \frac{1}{2} r \cdot S = \frac{1}{2} r \cdot H \cdot \left[\cot(\alpha - \frac{\varphi_h}{2}) - \cot(\alpha + \frac{\varphi_h}{2}) \right] \cdot \cos\theta \quad (15)$$

Assuming the frame rate r of 10 fps, the camera mounting height H of 5 meters, the tilt angle α of 30˚, the pan angle θ of zero degrees, and the angle of view φ defined by the sensor height h_s of 3.6 mm and the lens focal length f of 8 millimeters, we compute v_{max} as 191 km/h.

VIII. SHUTTER SPEED

If a vehicle crosses more than one pixel in the visual scene image M'N'Q'P', in Fig. 12, within the camera exposure time τ, its image will be blurred. For a vehicle moving at speed v, only the component parallel to the sensor plane, $v_s = v \sin\alpha$,can cause blur. This is shown in Fig. 15. In order to avoid blurs, the vehicle should move at a speed v_s such that, from Figs. 10 and 15,

$$\frac{v_s \cdot \tau}{d} \le \frac{\Delta}{f} \quad (16)$$

Where d is the distance of the vehicle from the camera, and Δ is the pixel size in the direction of the projected motion. For example, if the pan and roll angles to be zero, the vehicle moves across a colum of the sensor, and Δ is the pixel height.

$$V_s = V \sin\alpha \le \frac{\Delta \cdot d}{f \cdot \tau} = \frac{\Delta \cdot H}{f \cdot \tau \cdot \sin\alpha}$$

$$\tau \le \frac{\Delta \cdot H}{f \cdot V \cdot \sin^2 \alpha} \quad (17)$$

Assuming Δ to be 3.75 μm, the camera height H=5m, the focal length f=8mm, and the tilt angle α=30˚, the exposure time τ should be less than 177 μs, i.e. the shutter speed should be greater than 5660 Hz, for example 10,000 Hz.

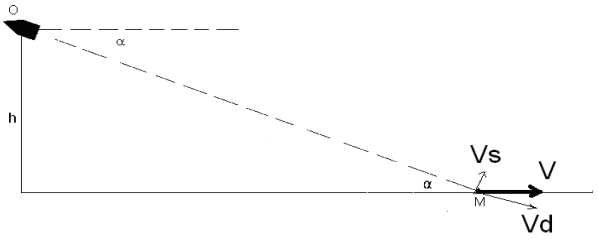

Figure 15. Setting the minimum shutter speed

IX. CONCLUSION AND RESULTS

The presented methodology in establishing camera intrinsic and extrinsic parameters has been applied to the design of a traffic enforcement system established in the city of Belgrade. The system consists of 14 control points equipped with cameras and a data processing center, as shown in Fig.16. It automatically detects vehicles infringing traffic light, bus lane and speed limit rules, identifies the infringing vehicle owners based on ALPR, and prepares traffic citations, Fig. 18. Two types of cameras and lenses are used: one for capturing the traffic violation, and the other for recognizing the license plate of the infringing vehicle. A set consisting of these cameras is shown in Fig. 17. The adopted methodology has shown to reduce the system design and installation time, and consequently the labor and equipment lease costs. Based on the first site survey, camera extrinsic and intrinsic parameters (such as focal length) was determined and tested on the ground before mounting on the gantry. In some cases, even a different camera choice based on necessary sensor size and resolution was suggested to cope with special requirements. This contrasts with the classical approach of adjusting manually camera settings at every site, which can take days, in comparison with hours when using our methodology.

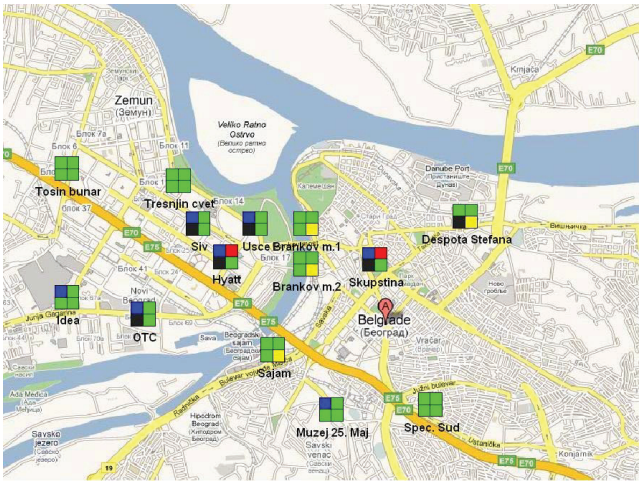

Figure 16. The traffic enforcement system has been installed on 14 locations in the city of Belgrade.

Figure 17. Two cameras are used in the system, one for ALPR (bottom), the other for traffic enforcement (top)

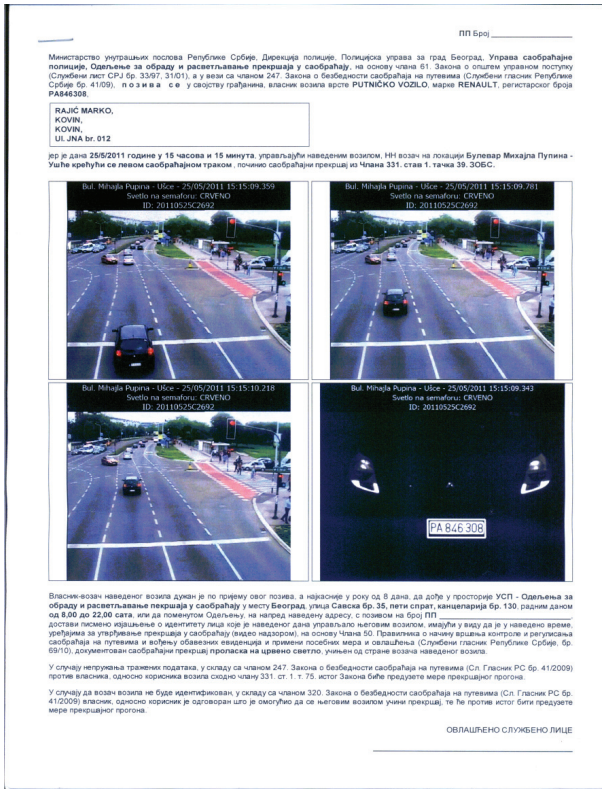

ПП Број _____

Министарство унутрашњих послова Републике Србије, Дирекција полиције, Полицијска управа за град Београд, **Управа саобраћајне полиције, Одељење за обраду и расветљавање прекршаја у саобраћају**, на основу члана 61. Закона о општем управном поступку (Службени лист СРЈ бр. 33/97, 31/01), а у вези са чланом 247. Закона о безбедности саобраћаја на путевима (Службени гласник Републике Србије бр. 41/09), **п о з и в а с е** у својству грађанина, власник возила врсте **PUTNIČKO VOZILO**, марке **RENAULT**, регистарског броја **PA846308**,

RAJIĆ MARKO,
KOVIN,
KOVIN,
Ul. JNA br. 012

јер је дана **25/5/2011 године у 15 часова и 15 минута**, управљајући наведеним возилом, НН возач на локацији **Булевар Михајла Пупина - Ушће крећући се левом саобраћајном траком**, почињено саобраћајни прекршај из **Члана 331. став 1. тачка 39. ЗОБС.**

Власник-возач наведеног возила дужан је по пријему овог позива, а најкасније у року од 8 дана, да дође у просторије **УСП - Одељења за обраду и расветљавање прекршаја у саобраћају** у месту **Београд**, улица **Савска бр. 35, пети спрат, канцеларија бр. 130**, радним даном **од 8,00 до 22,00 сата**, или да поменутом Одељењу, на напред наведену адресу, с позивом на број ПП _____ достави писмено изјашњење о идентитету лица које је наведеног дана управљало његовим возилом, имајући у виду да је у наведено време, уређајима за утврђивање прекршаја у саобраћају (видео надзором), на основу Члана 50. Правилника о начину вршења контроле и регулисања саобраћаја на путевима и вођењу обавезних евиденција и примене посебних мера и овлашћења (Службени гласник Републике Србије, бр. 69/10), документован саобраћајни прекршај **проласка на црвено светло**, учињен од стране возача наведеног возила.

У случају непружања тражених података, у складу са чланом 247. Закона о безбедности саобраћаја на путевима (Сл. Гласник РС бр. 41/2009) против власника, односно корисника возила сходно члану 331. ст. 1. т. 75. истог Закона биће предузете мере прекршајног прогона.

У случају да возач возила не буде идентификован, у складу са чланом 320. Закона о безбедности саобраћаја на путевима (Сл. Гласник РС бр. 41/2009) власник, односно корисник је одговоран што је омогућио да се његовим возилом учини прекршај, те ће против истог бити предузете мере прекршајног прогона.

ОВЛАШЋЕНО СЛУЖБЕНО ЛИЦЕ

_____

Figure 18. An automatically generated traffic citation

REFERENCES

[1] R. Y. Tsai, "A versatile camera calibration technique for high-accuracy 3D machine vision metrology using off-the-shelf TV cameras and lenses. IEEE Journal of Robotics and Automation RA-3(4): 323-344.

[2] Y. I. Abdel-Aziz,, H. M. Karara, "Direct linear transformation into object space coordinates in close-range photogrammetry", n Proc. of the Symposium on Close-Range Photogrammetry (1971), pp. 1-18

[3] Q.-T. Luong, O. Faugeras, The fundamental matrix: theory, algorithms, and stability analysis. The International Journal of Computer Vision , vol. 17, number 1, pages 43-76, January 1995.

[4] F. Peng, C. Liu, X. Ding, "Camera Calibration And Near-view Vehicle Speed Estimation" Proceedings of SPIE Vol. 6813, pp. 681314:1-10, January 2008.

[5] O. Faugeras,Q.T. Luong. The geometry of multiple images. MIT Press, 2001

[6] O. Faugeras, L. Robert. What can two images tell us about a third one? International Journal of Computer Vision, 18:5-19, 1996.

[7] R. Hartley, A. Zisserman. Multiple view geometry in computer vision. Cambridge University Press, 2nd Ed, 2004

[8] N.H.C. Yung, G.K.H Pang, S.K. Fung, "A Novel Camera Calibration Technique for Visual Traffic Surveillance", Proceedings of 7th World Congress on Intelligent Transport Systems, Turin, Italy, 2000

[9] N.J. Kanhere, S.T. Birchfield, "A taxonomy and analysis of camera calibration methods for traffic monitoring applications", IEEE Transactions on Intelligent Transportation Systems, Volume 11 Issue 2, pp 441-452, June 2010

[10] E.K. Bas, and J.D. Crisman, "An Easy to Install Camera Calibration for Traffic Monitoring," P*roceedings of IEEE Conference on Intelligent Transportation Systems*, pp. 362-366, 1997.

[11] M. Haralick, "Using Perspective Transformations in Scene Analysis," *Computer Graphics and Image Processing*, vol. 13, pp. 191-221, 1980.

[12] http://www.leewardpro.com/articles/licplatefonts/font-din1451.html

[13] X. Chen, L. Li, and Y. Zhang. "A markov model for headway/spacing distribution of road traffic," IEEE Transactions on Intelligent Transportation Systems, 11(4):773-785, 2010

[14] OBrien, E.J., Lipari, A. and Caprani, C.C. (2011), 'Estimation of density and gaps in congested traffic', Proceedings of the Irish Transportation Research Network 2011, ITRN2011, 31 August-1 September, Cork

[15] T. Trigs, W, Harris, Report on Reaction time of drivers to road stimuli. Department of Psychology, Monash University, Australia, June 1982, ISBN 0 86746 147 0

[16] A. P. Pentland, A new sense for depth of field, in IEEE Transactions on Pattern Analysis and Machine Intelligence, PAMI-9, Issue 4, pp. 523-531, July 1987